

RESEARCH ARTICLE

Optimization of flexo process parameters to reduce the overall manufacturing cost

Akshay V. Joshi *

Department of Printing Engineering, P. V. G's College of Engineering & Technology and G. K. Pate (Wani) Institute of Management, Pune, India
avj_print@pvgoet.ac.in

ARTICLE INFO

Article history:

Received: 12 July 2021

Accepted: 23 November 2021

Available Online: 2 January 2022

Keywords:

Flexography

Polyethylene

Design of Experiments

Analysis of Variance

Regression

AMS Classification 2010:

62K05 62K15, 62K86

ABSTRACT

The flexo process parameters play an important role in ink transfer and will lead to wastage of inks, substrate, solvents and printed stocks if not monitored and controlled. The work focuses on optimizing the flexo process parameters for 40 microns 3-layer polyethylene (PE) film with Blue Nitrocellulose (NC) ink to reduce overall manufacturing cost while maintaining the print quality for diaper application. An experimental design was conducted for the response Ink GSM (grams per square meter), ΔE and Print Mottle with factors such as ink viscosity, anilox volume, plate dot shape and substrate opacity. The data was analyzed through Main Effect, Interaction Plot and Analysis of Variance (ANOVA). The regression models were developed for the response to validate the predictive ability of model. The process optimization resulted in reduction of Ink GSM, ΔE and Print Mottle by 18%, 52% and 1% respectively. The ink consumption reduced by 18.26% with minimized print defects, thereby reducing the overall manufacturing cost.



1. Introduction

As per Mordor Intelligence Report [1], the growth of flexography printing market will be 2.44% CAGR within a period from 2021 to 2026 which accounts to 124.61 USD billion from 107.42 USD billion. A large part of the flexography industry clientele remains to be from the industry catering to the needs of people i.e. personal care products like baby diapers. The India Diaper Market Outlook 2021 [2] reports 22.23% CAGR in baby diaper market over past 5 years. There are almost 25 million babies born every year. The hygiene awareness of Indian mothers, rise in income of common people has led to an exponential growth in diaper market. These diapers are packaged in pouches that are printed on Polyethylene (PE) and Cast Polypropylene (CPP) films using NC based inks by Flexo process. The surface anomalies and print defects, plate fill-ups, frequent machine stoppages, shade inconsistency is one of the major challenges during printing these films. This results in print mottle, uneven print density and ink deposition, thereby depreciating the print quality and degrading the selling potential of the product. Furthermore, the overall manufacturing

cost inclusive of printing, converting and process scrap cost is high. This demands for optimization with tight control of flexo process parameters to minimize the total manufacturing cost with improved print quality.

2. Flexography printing process

Flexography is a printing process which utilizes a flexible relief plate that adheres to a printing cylinder. The usage of flexible (soft) printing plates and low viscosity inks prints on a wide range of absorbent and non-absorbent substrates such as plastics, metallic films, paper and board. These plates are mounted on sleeves that receive ink from the ink pan through an anilox roller. An anilox roller is a cylinder consisting of fixed number of cells with a definite volume. A doctor blade is used to control the amount of ink transferred to the anilox roller. It wipes out any extra ink is collected back to the ink tray. The anilox roller rotates in the ink tray and carries the ink in its cells to the flexible plate mounted on a sleeve. In this process, ink gets transferred from anilox roller to the raised areas of the plate and thus inking only the image portion. This image area then comes in contact with the substrate and

*Corresponding author

transfers the image onto it by thrusting itself against the impression roller (Figure 1). The pressure between the plate cylinder and the impression roller is termed as kiss pressure and should be just enough to transfer ink from plate to substrate [3].

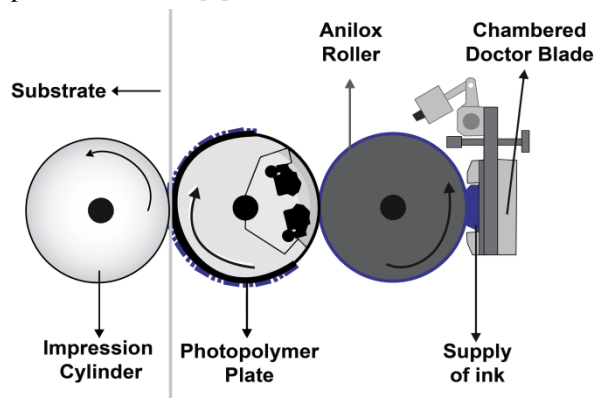


Figure 1. Flexography printing process

3. Flexography process parameters

The parameters that affect ink transfer in flexography and printability include plate, anilox, ink, substrate, solvents, press speed, surface energy of substrate etc. The printability attributes include density, Tone Value Increase, color deviation (Delta E), gloss, ink coat weight (GSM) and print mottle. Several works have been conducted by researchers to obtain the optimum print quality in the flexography print process [4-15]. The cost of print can be easily reduced by increasing the ink mileage and optimizing the flexo process parameters.

The anilox roller is the heart of flexography process and plays a significant role in ink transfer. The 60-degree hexagonal pattern are shallower and accommodates 15% more cells as compared to 30-degree hex, 45-degree tri-helical and 70-degree cell angles. The 60-degree hex cells provide better dot support during printing with greater uniformity [4]. The flexo ink transfer is directly proportional to the anilox roller cell volume [5]. A thinner ink film is deposited on the substrate at higher anilox line screen that carries more no. of cells in a given area. This results in less ink transfer due to cell clogging, anilox scoring, and anilox wear. The lower line screen and volume led to a smoother cell surface with consistent ink transfer and print performance. There exists a direct relation between the coating deposit and the volume of the anilox. The ink transfer is governed by type of anilox engraving techniques, inking system and plate-making. These parameters allow to accommodate finer screen volume with lower cell volume [6-9]. The ink film thickness in flexography process depends upon the anilox volume measured in billion cubic microns. The transfer of ink from anilox to plate is almost 50% and further transfers 50% of the ink from plate to the substrate [3, 10]. In order to avoid print defects such as dirty print and dot dipping, banded anilox test should be performed with varying anilox screen and cell volume to identify the right specification of anilox

roller for optimal ink transfer [11]. The laser engraved ceramic coated anilox roller has better release properties as compared to mechanically engraved chrome anilox roller. The quality of ink lay-down improves with ceramic coated anilox rollers [12]. The print consistency shall be achieved by the right selection of anilox screen ruling, volume and cell geometry [13].

The type of coating and polarity of substrate has a significant effect on print gloss and density. The coating on the substrate provides higher gloss as compared to uncoated substrate. The print density on uncoated substrate is inconsistent due to the ink deposition on the rough areas of the substrate. The presence of coating on the substrate leads to even lay-down of an ink. The print density increases with higher polarity of the substrate [14].

The ink film thickness and tone value increase in flexography is affected by the type of substrate, ink and viscosity. The print density increases for both solvent and water based flexo inks with the increase in anilox volume. The coated substrate reproduces higher print density with solvent-based inks as compared to water-based inks while the behavior is opposite for uncoated substrate. A higher tone value increase is noted with water-based ink on coated substrate as compared to solvent-based ink which is exactly opposite to uncoated substrate [15].

The solvents have a significant impact on the accuracy of the structures. The flexographic printing plate material must adapt to the solvents in functional fluids to avoid plate swelling due to penetration of solvents in plate [16]. The solvents used in flexographic ink play an important role in printed dot reproduction of both coated and uncoated paper. The dot shape improves with ink having high boiling point solvent and low drying velocity than the ink with low boiling point solvent and high drying velocity [17].

The ink transfer in flexography is governed by the substrate manufacturing processes. The correlation between substrate surface energy and ink surface tension have an impact on ink transfer. The surface treatments increase surface energy of the substrate that reduces the contact angle and improve wettability. The liquids adhere stronger to a surface with high surface energy [18]. The films with higher surface free energy results in higher optical density. A stronger adhesion leads to thicker layer of ink and hence higher optical density. The optical density is greatly affected by polar component of surface energy in water-diluted inks and dispersive component of free surface energy in solvent based inks [19]. The substrate with lower surface energy reduces wettability and results in higher mottle [20]. The non-uniform corona treatment will result in improper wetting on the printing surface and lead to occurrence of uncovered areas in the print [21]. The dot gain is affected by the nip pressure between plate and impression cylinder. The dot size increases with an increase in line screen [22]. The increased plate to

substrate engagement results in reduction in L^* values while higher anilox to plate pressure yields higher ink transfer in the mid-tone areas. The rise in press speed initially produces a drop in ink transfer but increases with further increased speed, particularly in the highlights [23]. The type of flexo plate-making has an impact on print quality. The digital plate-making shows significant improvement in print contrast and tonal values as compared to conventional photopolymer plate [24]. The increase in depth of dot, increases dot stability that results in reduced tone value increase. The dot is expanded with an engagement of printing cylinder and impression cylinder. The line rulings on plate affects the image quality if not compensated during pre-press [25].

3.1. Substrate-ink interaction

The substrate surface energy, ink surface tension and interfacial tension between substrate and ink dictates the printability in flexography.

3.1.1. Surface energy of substrate

The measure of break up of inter-molecular bonds occurring at the surface is referred to as surface energy. In simple terms, it is the energy required per unit area to increase the size of surface and measured in mN/m.

In the most basic sense, surface free energy is defined as the adhesive characteristic of the solid, indicating its affinity towards the other materials. The substrate surface energy and ink surface tension are the crucial factors in ink transfer, spreading and adhesion. The difference between the surface energy and the surface tension has larger impact on ink transfer and extent of spreading. Higher the difference lower will be contact angle and better is the ink spreading on the substrate. Nevertheless, very high surface energy may lead to erratic print quality.

Surface free energy can be calculated by contact angle measurement with certain liquids of known surface tension. Contact angle is the angle between a liquid surface and the outline of contact surface of solid. The contact angle of a drop of liquid over a solid surface is determined by Young's Equation. Young described the relation between surface energy of solids, surface tension of liquid and their interfacial surface tension. It is mathematically given by:

$$\cos\theta = (\gamma_S - \gamma_{LS})/\gamma_L \quad (1)$$

Where

θ = contact angle of liquid

γ_S = Surface Energy of Solid

γ_L = Surface Tension of Liquid

γ_{SL} = Interfacial Surface Tension between Solid and Liquid

The contact angle can be measured by either by varying the drop volume or with constant drop volume. The factors that affect contact angle other than substrate surface energy are ink surface tension, its viscosity and

wetting speed. The contact angle determines liquid's wettability on that surface. Thus higher the contact angle lower will be the wettability.

Two types of PE substrates were selected for the work having an average opacity of 79% and 82%. The surface energy of these substrates were determined by measuring the contact angle of two test liquids viz., Formamide and Glycerol of known polar and dispersive components. Holmarc Contact Angle Meter was used to measure contact angle on both the substrates with 10 samples each.

The geometric mean equation was used to calculate the surface energy of these substrates.

$$\gamma_{SL} = \gamma_S + \gamma_L - 2(\sqrt{\gamma_S^d \gamma_L^d} + \sqrt{\gamma_S^p \gamma_L^p}) \quad (2)$$

γ_S = Surface Energy of Solid

γ_L = Surface Tension of Liquid

γ_{SL} = Interfacial Surface Tension between Solid and Liquid

The above equation was replaced by simplified Young's Equation to calculate the surface energy from the contact angle.

$$\gamma_L(1 + \cos\theta) = 2[\sqrt{\gamma_L^d \gamma_S^d} + \sqrt{\gamma_L^p \gamma_S^p}] \quad (3)$$

Where

γ_S^d = dispersive component of solid

γ_L^d = dispersive component of liquid

γ_S^p = polar component of solid

γ_L^p = polar component of liquid

γ_S^d of Formamide = 39.5 γ_L^p of Formamide = 18.7

γ_L^d of Glycerol = 34 γ_L^p of Glycerol = 30

γ_L of Formamide = 58.2

γ_L of Glycerol = 64

Substrate 1

$$58.2(1 + \cos 67.51) = 2[\sqrt{39.5 \times \gamma_S^d} + \sqrt{18.7 \times \gamma_S^p}] \quad (4)$$

$$64(1 + \cos 80.78) = 2[\sqrt{34 \times \gamma_S^d} + \sqrt{30 \times \gamma_S^p}] \quad (5)$$

Solving equation (4) and (5), polar and dispersive components of substrate 1 was calculated

$\gamma_S^d = 42.05$ and $\gamma_S^p = 0.0225$

Therefore, Total Surface Energy of PE laminate for Substrate 1

= $\gamma_S^d + \gamma_S^p = 42.26$ mN/m

Substrate 2

$$58.2(1 + \cos 68.6) = 2[\sqrt{39.5 \times \gamma_S^d} + \sqrt{18.7 \times \gamma_S^p}] \quad (6)$$

$$64(1 + \cos 81.48) = 2[\sqrt{34 \times \gamma_s^d} + \sqrt{30 \times \gamma_s^p}] \quad (7)$$

The polar and dispersive component of Substrate 2 was hence calculated by solving equation (6) and (7).

$$\gamma_s^d = 40.70 \text{ and } \gamma_s^p = 0.00722$$

Therefore, total Surface Energy of PE laminate for Substrate 2

$$= \gamma_s^d + \gamma_s^p = 40.7 \text{ mN/m}$$

Substrate 1 and Substrate 2 are different in only opacity. The opacity of substrate was varied to check its effect on print attributes. Both the substrates are 40 μ thickness (37 GSM) with 0.943 density. The gloss of the substrates was 65% @ 60°. The Coefficient of Friction (CoF) was ranging between 0.3 to 0.4 while Haze between 10% to 15%.

3.1.2. Surface tension of ink

Table 1. Contact angle measurement

Viscosity @22°C (sec)	Left Angle (°)	Right Angle (°)	Contact Angle (°)
20	39.5	41.58	40.54
22	44.13	45.71	44.92
24	45.18	48.22	46.70

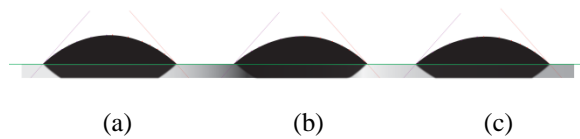


Figure 2. Contact angle (θ) 20 sec (a), 22 sec (b), 24 sec (c)

The contact angle was found to be lower at 20 sec viscosity (Table 1), thereby resulting in higher ink spread and print mottle (Figure 2).

Surface Tension is defined as the amount of energy required to increase the surface of the liquid by unit area. The surface tension was determined based on Wilhelmy Plate method [26].

$$\gamma = \frac{F}{l \cos\theta} \quad (8)$$

Where,

F = Force acting on the plate

γ = Surface tension of liquid (ink)

l = Wetted perimeter of the plate

θ = Contact angle with plate

Surface tension measurement was conducted on 10 samples of ink to increase accuracy of measurement. The mean surface tension was found to be 23.98mN/m at 22°C. The temperature is a crucial factor affecting surface tension. The rise in temperature exerts more molecular vibrations among the liquid molecules, thereby decreasing surface tension. The increase in temperature, increases adhesion and decreases the

cohesive forces between liquid molecules. This results in increased contact angle and reduced surface tension. The ink-substrate interaction is critical to print quality. The ink lay-down over the substrate after transfer from the plate has an impact on printability. The ink spreading depends on various printability factors such as circularity, area and perimeter of the dot. Moreover, it reflects directly on print defects such as voids and print mottle. A higher spreading tendency of ink over the substrate leads to better area coverage, reducing void area. On the contrary, spreading yields in scattered distribution of pigment particles with uneven reflectance from the printed substrate, thus leading to higher print mottle over non-absorbent substrates. NC based ink was prepared in a dispenser that comprised of Master Batch, Varnish/Resin, Medium and Solvent. Master Batch is a combination of Pigment, Additives, Varnish and True Solvent (Table 2).

Table 2. Basic composition of NC ink

Ingredients	Proportion (%)
Master Batch	42% - 52%
Vanish	24% - 26%
Medium	5% - 10%
Solvent	17% - 24%
Total	100%

Table 3. Substrate-ink interaction

Substrate Opacity	η (s)	(θ)	γ _s	γ _l	γ _{sl}	W _a	S
Substrate 1 (79%)	20	37	42	24	23	43	-4.9
	22	42	42	24	24	42	-6.0
	24	45	42	24	25	41	-6.9
Substrate 2 (82%)	20	41	41	24	23	42	-5.8
	22	45	41	24	24	41	-7.0
	24	47	41	24	25	40	-7.5

The interfacial tension (γ_{sl}), work of adhesion (W_a) and spreading co-efficient (S) was calculated using following formulae:

$$\gamma_{sl} = \gamma_s - \gamma_l(\cos\theta) \quad (9)$$

$$S = \gamma_s - \gamma_l - \gamma_{sl} \quad (10)$$

where θ = Contact angle of ink with substrate.

The values of contact angle from Table 3 suggest higher spreading at lower ink viscosity (20 sec) for both the substrates. The higher surface energy of substrate 1 increases the ability of the substrate to bind with ink. Higher surface energy ensures higher spreading as the amount of spreading is directly proportional to the difference in substrate surface energy of substrate and ink surface tension. This difference is found to be greater in substrate 1 and hence the ink spread is more in substrate 1 than substrate 2. Furthermore, the lower contact angle at lower viscosity resulted in higher ink spread and print mottle. A higher adhesion between the

ink and substrate is achieved on substrate 1 as indicated by higher work of adhesion (w_a). The negative values of spreading co-efficient (S) suggest that the spreading does not occur spontaneously. Substrate 2 displayed lower ink spread indicated by higher magnitude of S . Thus, 20 sec ink viscosity on substrate 1 resulted in higher ink spread.

4. Printability analysis

Printability is essential for defining the optimum settings for improving print quality in flexography printing press. Printability in this study is defined as the optimal amalgamation of ink, substrate and process parameters for the responses such as ink gsm (grams per square meter), ΔE^*00 and print mottle. The optimization of these responses with minimized defects shall enhance printability and reduce the overall manufacturing cost of a package.

4.1. Plate dot structure

Two plates, with dot structure 1 (circular) and dot structure 2 (square) were used for the study. The plate layout design comprised of logo, solid and halftone patch, surface and reverse text. The solid patch was included to measure and analyze Ink GSM, ΔE^*00 and Print Mottle. The halftone patch was used to check the tone value increase. The logo was incorporated in the layout for visual assessment while surface and reverse text to check minimum reproducible text. These plates were mounted on the same sleeve and printing was carried out by keeping the other color parameters constant.

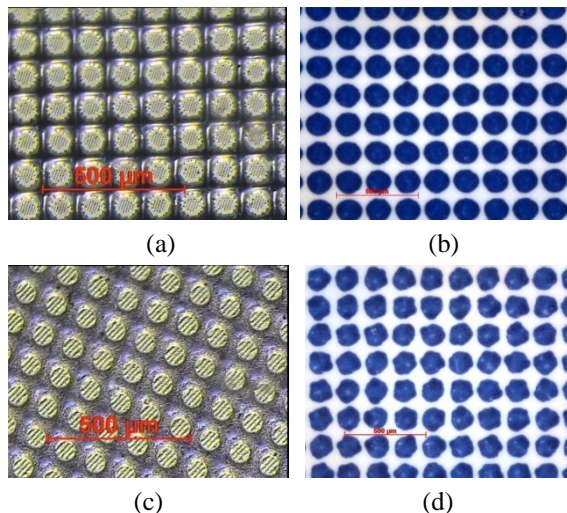


Figure 3. Dot shape on Plate 1 (a), Dot reproduction of Plate 1 (b), Dot shape on Plate 2 (c), Dot reproduction of Plate 2 (d).

The dot circularity also referred to as roundness and represented as

$$C = \frac{4\pi A}{P^2} \quad (11)$$

where A = area of dot and P = perimeter of the dot

The ideal dot circularity is 1 and more closer to 1, better is the dot reproduction. The dot circularity of Dot Shape

1 (0.8194) was found to be higher than Dot Shape 2 (0.8163) as indicated by Figure 3.

4.2. Baseline identification

A production run was conducted on 40μ PE substrate with solvent based blue ink at 23s ink viscosity (30°C and 50% humidity) as measured by B4 Ford cup and diluted with n-propanol and n-propyl acetate in the ratio of 4:1. A anilox cell volume of 5.3 billion cubic microns (BCM), square dot plate and 79% average substrate opacity was used for the run. The other constant parameters set during the press run were 5.83 m/s press speed, 1.7 mm plate thickness, medium backing tape with 0.38 mm thickness and 30° reverse angle chambered doctor blade. The assessment of response Ink GSM, Color Deviation (ΔE^*00) and Print Mottle was done with 20 printed sheets being considered as sample size for each response. The baseline for Ink GSM and Print Mottle was the mean value of the sample size. The baseline or reference $L^*a^*b^*$ values for the blue color was 14.42L* 36.22a* -66.53b* and the target was set to reduce the color deviation from the baseline for the printed blue sample with ΔE^*00 not exceeding 1.5 (Table 4).

Table 4. Baseline for the response

Run	Ink GSM	ΔE^*00	Print Mottle
Production Run	0.98	1.07	0.91

The selection of anilox roller cell volume was based on ratio of plate to anilox screen ruling and the available inventory used in daily production run. The plate to anilox screen ruling was kept in a range of 1:5 (5.3 BCM) and 1:7 (4.5 BCM) with plate screen ruling as 133 lpi while anilox screen ruling as 648 lpi and 914 lpi.

Table 5. Design of experiments for the response

Factors	Low	Mid	High
	Level	Level	Level
Viscosity (sec)	20	22	24
Anilox Volume (BCM)	4.5	-	5.3
Dot Shape	1	-	2
Substrate Opacity (%)	1	-	2

A general full factorial experimental design was run with 4 factors namely viscosity with 3 levels while anilox volume, dot shape and substrate opacity at 2-levels and 2 replicates, thus totaling to 48 runs (Table 5). The dot shape 1 refers to dot circularity of 0.8194 while dot shape 2 refers to dot circularity of 0.8163. The lower level of substrate opacity represents mean opacity of 79% while higher level represents mean opacity of 82%. The selection of levels for the factors in DOE were considered based on the working levels. A viscosity lower than 20 sec will result in more tone value increase and mottling while viscosity above 24 sec will clog the anilox cells and yield in uneven lay down of an ink. Anilox volume levels were considered

based on ratio of plate to anilox line screen. There are only two types of dot shape available round and square, hence considered. The recommended substrate opacity for the diaper application is normally ranging between 80% to 82%. The substrate opacity below 79% will result in dispersion lines on PE substrate while opacity above 82% will require more addition of master-batch, thereby increasing the production cost. Hence, the two opacity levels of 79% and 82% were considered for the work.

4.3. Ink GSM

Ink GSM is the amount of ink deposited over one square meter of printed substrate. The Ink GSM was measured on solid patch of the printed sample.

The main effect plot (Figure 4) shows that higher ink GSM is obtained at higher viscosity (24 sec) and anilox volume (5.3 BCM) with a circular dot (dot shape 1) on lower substrate opacity. The solid content in the ink is higher at 24 sec viscosity that constitutes higher ink GSM. The anilox volume determines the quantity of ink transfer to the plate and further on to the substrate. Higher the anilox volume, higher the amount of ink deposited and therefore the ink GSM. The larger area coverage on plate with dot shape 1 (circular dot) led to higher ink transfer and ink GSM. The difference between substrate surface energy and ink surface tension played a significant role in ink transfer. The substrate 1 with higher surface energy showed higher difference that led to more ink transfer. A higher surface energy increases the force of adhesion between the ink and the substrate. This force of adhesion pulls more ink from the plate and hence results in a higher ink GSM.

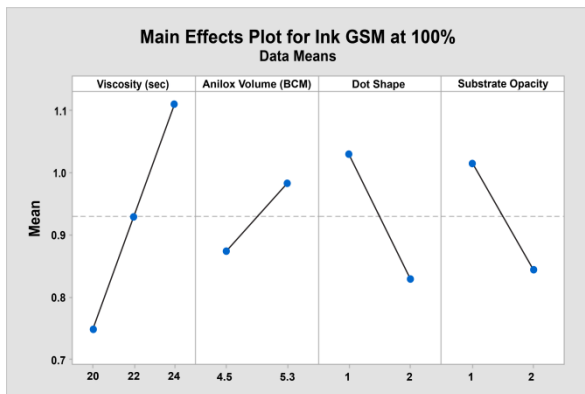


Figure 4. Main effect plot for ink GSM

There is no strong interaction between the factors affecting ink GSM (Figure 5). High ink GSM is obtained when an ink having 24 sec viscosity is used irrespective of the plates, anilox volume and substrate used. Similarly anilox volume of 5.3 BCM, dot shape-1 and substrate opacity-1 yielded maximum ink GSM. Minitab 17 was used to calculate ANOVA (Analysis of Variance) and Regression models for Ink GSM, ΔE and Print Mottle.

The degrees of freedom abbreviated as df (Table 6) are the number of values that can be varied once certain parameters have been established.

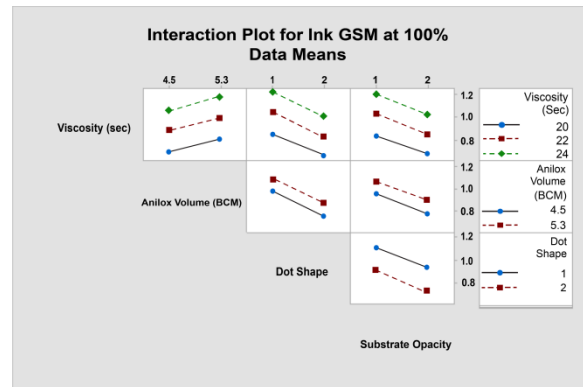


Figure 5. Interaction plot for ink GSM

Table 6. ANOVA for ink GSM

Source	df	Adj SS	Adj MS	F	P
Regression	7	2.030	0.29	2222.15	0.000
Viscosity (sec)	1	1.048	1.048	8024.92	0.000
Anilox Volume (BCM)	1	0.146	0.146	1120.69	0.000
Dot Shape	1	0.486	0.486	3722.94	0.000
Substrate Opacity	1	0.349	0.349	2669.56	0.000
Viscosity* Dot Shape	1	0.0009	0.0009	6.92	0.012
Viscosity* Substrate Opacity	1	0.0007	0.0007	5.39	0.025
Dot Shape * Substrate Opacity	1	0.0006	0.0006	4.61	0.038
Error	40	0.0052	0.0001		
Lack of Fit	16	0.0021	0.0001	0.91	0.568
Pure Error	24	0.0033	0.0001		
Total	47	2.0358			
		S=0.0114257	R-sq =99.74%		
		R-sq(adj)= 99.70%	R-sq(pred)= 99.63%		

Adjusted Sum of Squares (Adj SS) are measures of variation for different components of the model. Sum of Squares describe the variation due to different sources. Adjusted Mean Square (Adj MS) measures the description of magnitude of variation by the term or model. Adj MS takes into consideration df. The F-value is the test statistic used to determine whether the term is associated with the response. It is the ratio of two sample variances i.e. MS of a particular row divided by MS Error. The p-value is the probability that measures the evidence against the null hypothesis. The lower p-values provide the stronger evidence against null hypothesis. The constants of the regression equation was derived from the coefficients of each term namely Viscosity, Anilox Volume, Dot Shape, Substrate Opacity and interactions between them.

Regression Equation for Ink GSM

$$\begin{aligned} InkGSM = & -1.542 + 0.10547Viscosity(sec) \\ & + 0.13802AniloxVolume (BCM) \\ & -0.0631DotShape - 0.046SubstrateOpacity(\%) \\ & -0.00531Viscosity*DotShape \\ & -0.00469Viscosity*SubstrateOpacity \\ & -0.01417DotShape*SubstrateOpacity \end{aligned} \quad (12)$$

The p-values in ANOVA (Table 6) of all the main factors are below α value of 0.05, thereby indicating as significant factors affecting Ink GSM. The lower p-values below α value of 0.05 proves rejection of null hypothesis. The viscosity was found to be of highest significance affecting Ink GSM as indicated by higher F-value. A 99.74% of variability could be explained by the model as indicated by R-Sq. value. The adjusted R-Sq of 99.70% shows significant improvement of the model with selected four factors. As the experimental design involved 2 replicates i.e. having multiple observations with an identical X values, hence lack-of-fit test was performed. The p-value greater than $\alpha > 0.05$ indicates that model correctly specifies the relationship between the response and predictors and the test does not detect lack-of-fit. The model was adequate as the lack of fit (p=0.568) value was greater than $\alpha > 0.05$.

4.4. Print density

The print density is directly correlated to ink GSM and therefore the trend for Ink GSM and print density is same as indicated by Main Effect Plot.

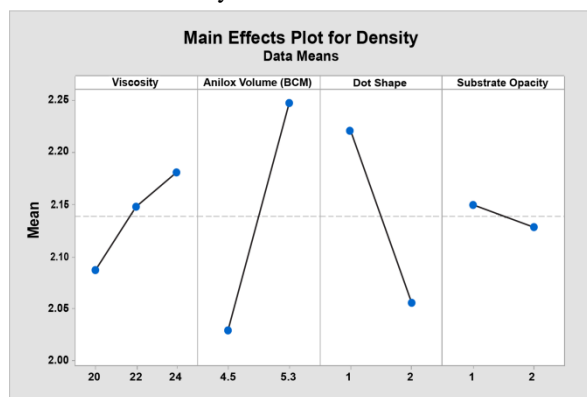


Figure 6. Main effect plot for print density

The main effects plot (Figure 6) shows that higher print density is obtained at higher viscosity, higher anilox volume, a circular dot shape and on a surface with lower opacity. A lower viscosity (20 sec) implies a lower concentration of solid content and hence a lower print density was achieved. A lower anilox volume (4.5 BCM) resulted in a lower print density. This occurred due to the fact that a lower anilox volume will store a less amount of ink and therefore will transfer lesser ink and hence a low print density. The dot shape 1 i.e. circular dots exhibited higher print density than square dotted plate. This can be attributed to the fact that area

coverage of circular dot is more than square dot (dot shape 2) and transfers more ink as compared to a square dot. The substrate 1 with lower mean opacity of 79% displayed a higher print density than substrate 2 i.e. mean opacity of 82.4%. A higher ink transfer was observed at lower substrate opacity 1 due to higher surface energy of 42.26mN/m as compared to higher substrate opacity with a lower surface energy of 40.7mN/m that has led to higher print density.

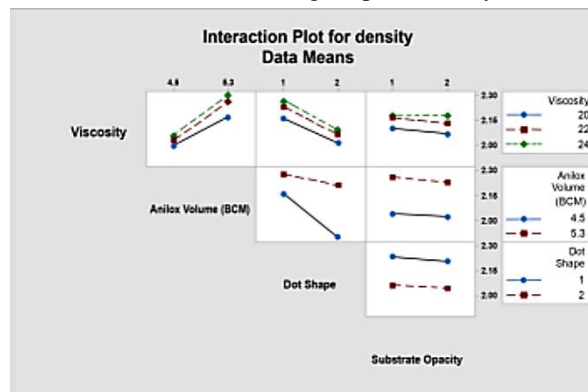


Figure 7. Interaction plot for print density

The interaction plot for density (Figure 7) shows higher density at 24s viscosity, 5.3 BCM anilox volume for a circular dot shape at lower substrate opacity. The interaction of viscosity with anilox volume, dot shape and substrate opacity affects the print density. The higher solid content at 24 sec ink viscosity and more ink carrying capacity of 5.3 BCM anilox volume resulted in high ink deposition on to the substrate; thereby higher print density. The higher area coverage of plate dot 1 and higher viscosity of 24 sec with less ink spread yielded in higher ink film thickness, thus higher print density. The ink with higher viscosity, high anilox BCM and circular dots yield high print densities. The interaction plot shows great inter dependence of circular dots with anilox volume. A sharp rise in print density was observed with circular dots at 4.5 BCM anilox volume as compared to square dots. The higher ink transfer at lower substrate opacity with higher surface energy was achieved at 24 sec ink viscosity.

4.5. Delta E

The color variation or deviation in the print is referred to as Delta E. It involves a 3 dimensional color space where each color occupies unique location according to its color co-ordinates namely L^* , a^* and b^* . The L^* refers to lightness and darkness of a color. The a^* refers to green and red coordinates while yellow and blue coordinates are represented by b^* values.

$$\begin{aligned} \Delta E_{2000} &= \sqrt{\left(\frac{\Delta L'}{K_L S_L}\right)^2 + \left(\frac{\Delta C'}{K_C S_C}\right)^2 + \left(\frac{\Delta H'}{K_H S_H}\right)^2} + R_T \left(\frac{\Delta C'}{K_C S_C}\right) \left(\frac{\Delta H'}{K_H S_H}\right) \end{aligned} \quad (13)$$

Where,

$$\bar{L}' = (L_1 + L_2)/2$$

$$C_1 = \sqrt{a_1^2 + b_1^2}, \quad C_2 = \sqrt{a_2^2 + b_2^2}$$

$$\bar{C} = (C_1 + C_2)/2$$

$$G = \frac{1}{2} \left(1 - \sqrt{\frac{C^{-7}}{C^{-7} + 25^7}} \right)$$

$$a'_1 = a_1(1 + G), \quad a'_2 = a_2(1 + G)$$

$$C'_1 = \sqrt{a_1'^2 + b_1^2}, \quad C'_2 = \sqrt{a_2'^2 + b_2^2}$$

$$\bar{C}' = (C'_1 + C'_2)/2$$

$$\Delta L' = L_2 - L_1, \quad \Delta C' = C'_2 - C'_1$$

$$\Delta H' = \sqrt{C'_1 C'_2} \sin(\Delta h'/2)$$

$$S_L = 1 + \frac{0.015(\bar{L}' - 50)^2}{\sqrt{20 + (\bar{L}' - 50)^2}}$$

$$S_C = 1 + 0.045\bar{C}', \quad S_H = 1 + 0.015\bar{C}'T$$

$$\Delta\theta = 30 \exp\left\{-\left(\frac{H' - 275^\circ}{25}\right)^2\right\}$$

$$R_C = \sqrt{\frac{\bar{C}'^{17}}{\bar{C}'^{17} + 25}}, \quad RT = -R_C \sin(2\Delta\theta)$$

$$K_L = 1 \text{ default}, \quad K_C = 1 \text{ default}, \quad K_H = 1 \text{ default}$$

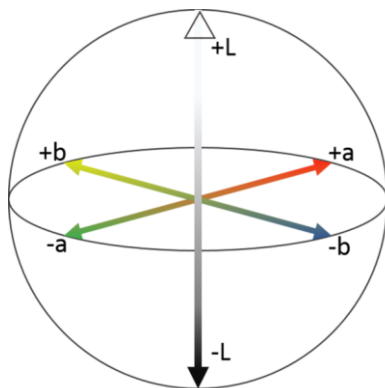


Figure 8. Lab color space

The color values of 14.42L* 36.22a* -66.53b* was considered as reference based on the customer approval. The color deviation was calculated based on CIE ΔE2000 (weighing factor 1:1:1) with M1 measurement mode, D50 illuminant and 2° observer angle between reference L*a*b* and L*a*b* values of printed samples measured on the solid patches. The Main Effect plot (Figure 9), depicts lower delta E at higher viscosity and anilox volume with square dot on higher substrate opacity. The plot (Figure 10) indicates an interaction of viscosity with anilox volume and dot shape affecting ΔE*00.

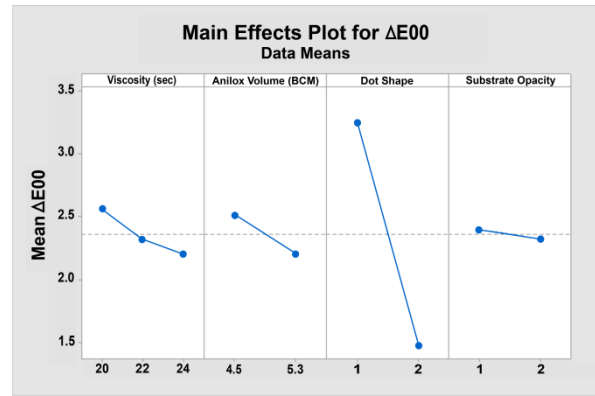


Figure 9. Main effect plot for ΔE*00.

The variation in ΔE2000 was due to the deviation in L* a* b* coordinates.

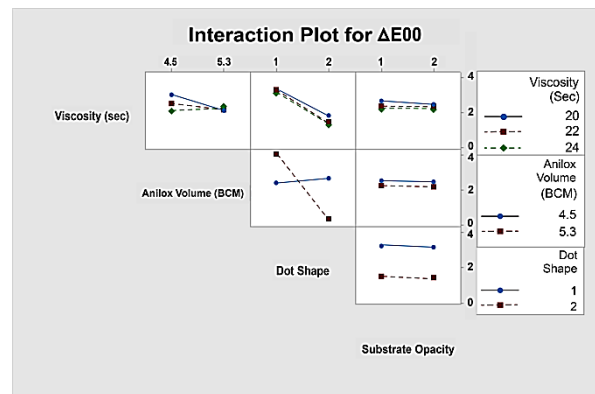


Figure 10. Interaction plot for ΔE*00

Table 7. ANOVA for ΔE00

Source	df	Adj SS	Adj MS	F	P
Regression	5	90.435	18.087	297.47	0.000
Viscosity (sec)	1	2.7209	2.7209	43.85	0.000
Anilox Volume (BCM)	1	0.0113	0.0113	0.18	0.671
Dot Shape	1	41.1262	41.1262	662.74	0.000
Viscosity* Anilox Volume	1	2.4753	2.4753	39.89	0.000
Anilox Volume*Dot Shape	1	48.1001	48.1001	775.12	0.000
Error	42	2.6063	0.0621		
Lack of Fit	18	1.5767	0.0876	2.04	0.051
Pure Error	24	1.0296	0.0429		
Total	47	93.0411			

S=0.249108 R-sq =97.20%

R-sq(adj)= 96.87% R-sq(pred)= 96.42%

Regression Equation for ΔE^*00

$$\begin{aligned} \Delta E^*00 = & 9.57 - 1.792 \text{Viscosity}(\text{sec}) - \\ & 0.53 \text{AniloxVolume}(\text{BCM}) + 22.753 \text{DotShape} \\ & + 0.3477 \text{Viscosity} * \text{AniloxVolume} \\ & - 5.005 \text{AniloxVolume}(\text{BCM}) + 22.753 \text{DotShape} \end{aligned} \quad (14)$$

The constants of the regression equation were derived from the coefficients of each factor and their interactions with each other. The ANOVA Table (Table 7) shows that all the main effects and interaction of viscosity with anilox volume, dot shape and anilox volume with dot shape as significant factors affecting Delta E. Dot shape was had an influential role in minimizing Delta E. The model summary indicates 97.20% of variability explained by the model while 96.8% adjusted R-Sq implies significant improvement of the model by using four factors. The lack of fit with p value of 0.051 represents the accuracy of the model.

4.6. Print mottle

Print Mottle is defined as the undulations present on the surface of substrate. Verity IA Print Target v3 software with Stochastic Frequency Distribution Analysis (SFDA) algorithm was used to measure Mottle on the solid patch. The output result of this algorithm is an index, quantifying mottle. SFDA firstly determines the properties of the texture of the image and then calculates the spatial distribution of the texture. When the scanned image area in digital format is fed to SFDA for analysis, the entire image area is sampled into a regular pattern of continuous and adjoining larger target areas which are further sub-divided into smaller pixel targets (Figure 11). The larger targets are measured for two parameters stored in separate databases simultaneously; one database stores the two-dimensional standard deviation (s) within the smaller target area while the second database stores the mean luminance value (M_{TL}) of the pixels present in the smaller target area that describes the overall visual impact of the analyzed larger target area. When an area of interest is selected within the scanned image, the s and M_{TL} values are extracted from their databases and the mottle index for the respective area of interest is displayed as a result.

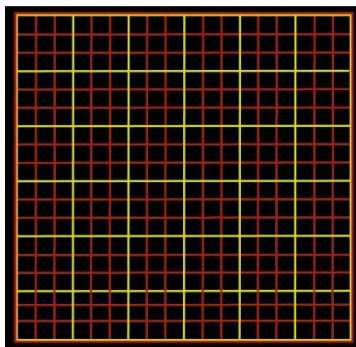


Figure 11. Area of interested divided into target areas

The standard deviation “s” is calculated as:

$$s = \sqrt{\frac{\sum(P_L - M_{TL})^2}{n}} \quad (15)$$

Where,

P_L -Individual pixel luminance

M_{TL} -Mean luminance of the pixels in the target area

n -Number of pixels in the target.

The level of uniformity among the targets is indicated by the degree of variation in the value of “s” while the uniformity in luminance is indicated by the variance of “ M_{TL} ”.

The mottle of the larger target is then calculated using the following formula.

$$\text{Mottle} = K * (\sigma_s * M_s * \sigma_m) \quad (16)$$

Where,

K -Scaling Factor,

σ_s -Standard deviation of s values

σ_m -Standard deviation of M_{TL} values

M_s -Mean of “s” values

The variation in the texture of image also needs to be calculated for more accurate mottle measurement. For calculating the mottle index of the entire area of interest, spatial distribution of texture mottle is calculated between the larger targets, by the following formula:

$$\text{SpatialMottle} = K * (\sigma_o * M_o) \quad (17)$$

σ_o = Standard deviation of large target mottle number

M_o = Mean of large target mottle number

The Print Mottle was measured on solid patch of the printed sample. The solid print mottle was minimized at higher level of viscosity (24 sec), anilox volume (5.3 BCM), substrate opacity and lower level of dot shape (Figure 12). The higher ink spreading at lower viscosity (20 sec) due to higher spreading coefficient of ink results in uneven ink deposition on the substrate, thereby leading to higher print mottle.

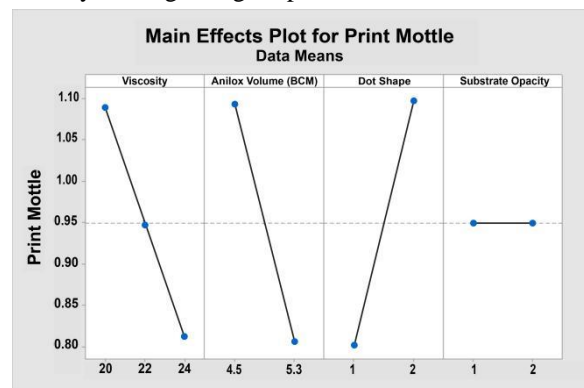


Figure 12. Main effect plot for print mottle

The even lay down of ink on the substrate at higher viscosity (24 sec) reproduces good dot circularity, thereby resulting in lower print mottle. Too higher viscosity will result in higher print mottle due anilox cell clogging. The outcome of this result will be uneven deposition of ink on the substrate. The print mottle was

reduced at higher anilox volume and circular dot (dot shape 1) due to higher and uniform ink film deposition. Though the print mottle was minimized with higher opacity substrate but the difference between both the substrate was negligible. This is because of lower surface energy of substrate 2 that led to less ink spread as compared to substrate 1.

The interaction plot (Figure 13) shows lower solid mottle at 24 sec viscosity, 5.3 BCM anilox volume with a circular dot on 82% mean substrate opacity. The interaction of lower anilox volume and lower viscosity yields a high mottle index. The higher solvent content at lower viscosity (20 sec) with lower anilox volume (4.5 BCM) results in uneven ink deposition on to the substrate, thereby higher print mottle. The lower dot circularity at lower viscosity with square dot leads to uneven distribution of ink on the substrate, thereby resulting in higher solid mottle. There was no significant interaction of substrate opacity with other factors and hence was not responsible for any change in solid mottle.

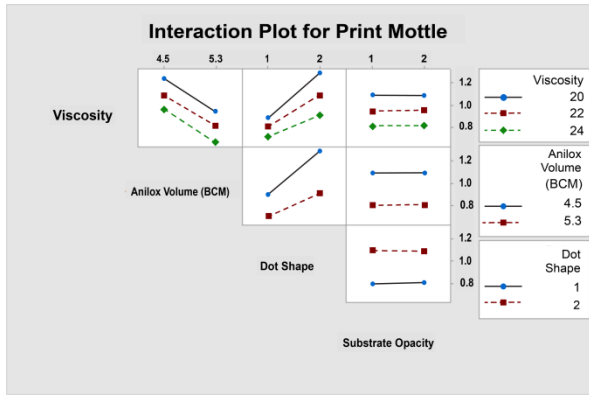


Figure 13. Interaction plot for print mottle

Table 8. ANOVA for print mottle

Source	df	Adj SS	Adj MS	F	P
Regression	5	2.827	0.56531	4829.11	0.000
Viscosity (sec)	1	0.611	0.6105	5215.23	0.000
Anilox Volume (BCM)	1	0.989	0.989	8448.42	0.000
Dot Shape	1	1.0355	1.0355	8845.42	0.000
Viscosity*Dot Shape	1	0.0861	0.0861	735.61	0.000
Anilox Volume *Dot Shape	1	0.1055	0.1055	900.95	0.000
Error	42	0.0052	0.0001		
Lack of Fit	18	0.0025	0.0001	1.34	0.247
Pure Error	24	0.0024	0.0001		
Total	47	2.3148			

S=0.0108196 R-sq =99.83%
R-sq(adj)= 99.81% R-sq(pred)= 99.78%

Regression Equation for Print Mottle

$$\text{Print Mottle} = 0.3250 + 0.00875\text{Viscosity(sec)} - 0.0073\text{AniloxVolume(BCM)} + 2.5384\text{DotShape} - 0.05188\text{Viscosity} * \text{DotShape} - 0.23438\text{AniloxVolume} * \text{DotShape} \quad (18)$$

The regression constants were derived from the coefficients of factors Viscosity, Anilox Volume, Dot Shape and the interactions of Dot Shape with Viscosity and Anilox Volume. Table 8 indicates that viscosity, anilox volume and dot shape along with their interactions have significant effect on minimizing print mottle. The lack of fit with p value of 0.247 represents model adequacy.

The regression equations for Ink GSM, Delta E and Print Mottle were validated by conducting additional runs. The data between Actual and Predicted runs showed R² value of 0.9242, 0.9372 and 0.9226 for Ink GSM, Delta E and Print Mottle respectively; hence justifying the predictive ability of the models.

4.7. Response optimization

The paramount settings for all the print attributes were optimized from the trials conducted as per the experimental design through response optimizer to identify the set of variables for multiple responses. The optimal settings for a single response are evaluated by individual desirability while composite desirability for multiple responses in the range of zero to one. The individual desirability will be 1 if the predicted response is closer to the target. The combination of individual desirability is calculated into an overall value as composite desirability for multiple responses. The higher the composite desirability value, the better the product quality. The response optimizer provides the "best" combination of variable settings as the global solution. The goal was set to minimize the response such as print mottle, ink GSM, and delta E. The composite desirability was estimated at different levels of anilox cell volume (BCM), viscosity, dot shape, and substrate opacity to identify the sweet spot between parameters fulfilling the goal.

The desirability to minimize a response is calculated as below.

$$d_i = 0 \quad (\bar{y}_i > U_i) \quad (19)$$

$$d_i = ((U_i - \bar{y}_i)/(U_i - T_i))^{n_i} \quad (yT_i \leq \bar{y}_i \leq U_i) \quad (20)$$

$$d_i = 1 \quad (\bar{y}_i < T_i) \quad (21)$$

Where,

\bar{Y}_i = predicted value of ith response

T_i = target value for ith response

U_i = highest acceptable value for ith response

d_i = desirability for ith response

Individual Desirability = (Upper value – Predicted response)/(Upper value – Target)

Composite Desirability,

$$D = (d_1 * d_2 * \dots * d_n)^{1/n} \quad (22)$$

Where

n = number of responses

D = Composite Desirability

The optimization plot (Figure 14) revealed global solution as 22 viscosity, 5.3 BCM anilox volume, dot shape 2 (square) having 82% substrate opacity (2) with 0.9726 composite desirability for minimization of Ink GSM, Delta E and Print Mottle on 40µ PE film.

The optimized settings with 22 sec viscosity, 5.3 BCM anilox cell volume, dot shape 2 (square dot) and 82% substrate opacity was run and average data of 20 printed sheets was considered.

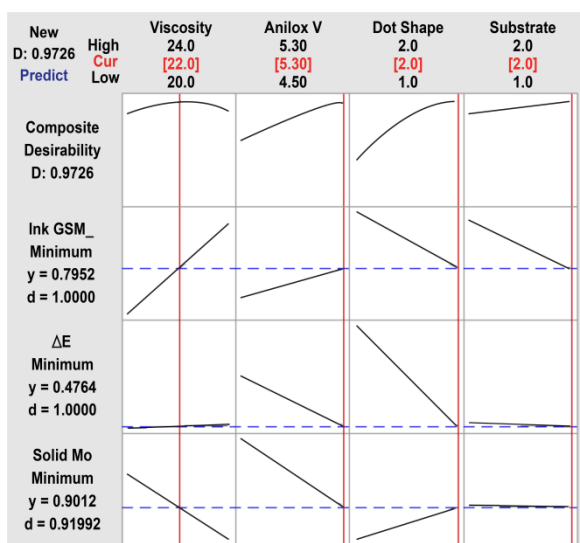


Figure 14. Optimization plot for the responses

Table 9. Comparison of the mean-field predictions

Response	Base-line	Optimized Run	% Improvement
Ink GSM	0.98	0.8	18
ΔE00	1.07	0.48	52
Print Mottle	0.91	0.9	1

The results revealed reduction of Ink GSM, ΔE00 and Print Mottle by 18%, 52% and 1% respectively (Table 9).

Table 10. Ink consumption

Runs	Ink Consumption per Area	Ink Consumption per KG	Ink Consumption per Tonne	% Improvement (Ink Consumption)
Production	0.23	25.99	25990	
Optimized	0.19	21.24	21240	18.26%

The area of one repeat of the job was 0.23 m² and accommodates 113 repeats/prints in a Kg. An Ink GSM of 0.98 was achieved during the production run while 0.80 for optimized run. The ink consumption per 0.23

m² for production run was 0.23 gm while 0.19 gm for optimized run. Table 10 shows minimization in ink consumption by 18.26% at optimized run of 22s viscosity and 5.3 BCM anilox volume with square dot plate (dot shape 2) on 40µ PE film a substrate having mean opacity 82% (substrate opacity 2).

5. Conclusion

A general full factorial DOE was designed to optimize flexo process parameters. The process parameters considered for experimentation were anilox volume (BCM) and dot shape at two levels while ink viscosity at three levels for both the substrates having mean opacity of 79% and 82%. The analysis of the data was assessed by main effects, interaction plot and ANOVA to determine the best combination of flexo process parameters enhancing printability. Furthermore, regression models were generated for the output response Ink GSM, Delta E, Print Mottle and validated. The validation runs for Ink GSM, Delta E and Print Mottle revealed good predictive ability of the models with R² value of 0.9242, 0.9372 and 0.9226 respectively. The results revealed that ink viscosity, anilox volume, dot shape and substrate opacity were significant factors affecting the response. The other factors such as a press speed, plate type, plate thickness, backing tape, doctor blade angle will also have a significant impact on ink transfer, thereby affecting the responses. The Response Optimizer revealed the optimized settings as 22 sec viscosity, 5.3 BCM anilox cell volume, dot shape 2 (square dot) and 82% mean substrate opacity on 40µ polyethylene film. However, the same methodology can be applied for other inks to validate the results for optimization and ink consumption. The optimal settings minimized the ink consumption by 18.26% while maintaining the desired ΔE*00 and reduction in overall manufacturing cost of a package.

Acknowledgments

The author would like to thank Parakh Flexipacks and Windmüller & Hölscher India Private Limited for their infrastructure and financial support.

References

- [1] Mordor Intelligence Report (2020). Flexible Plastic Packaging Market by Type (Pouches, Rollstocks, Bags, Wraps), Material (Plastic & Aluminum Foil), Application (Food, Beverage, Pharma & Healthcare, Personal care & Cosmetics), Technology, and Region - Global Forecast to 2025 [online]. Available from: <https://www.marketsandmarkets.com/Market-Reports/flexible-packaging-market-1271.html>. [Accessed 20 May 2021].
- [2] Indian Diaper Market (2016). India Diaper Market Overview, 2016 - Research and Markets [online]. Available from: <http://www.businesswire.com/news/home/20161128005918/en/India-Diaper-Market-Overview-2016---Research>. [Accessed 20 May 2021].
- [3] Kipphan, H. (2001). Handbook of Print Media.

- Springer-Verlag, Heidelberg, Berlin.
- [4] Rogers A. (2011). Choosing the right anilox-roll engraving for the application [online]. Available from: http://www.harperimage.com/media/downloads/Choosing%20the%20right%20engraving_Converting%20Q%204thQtrr2011.pdf. [Accessed 20 May 2021].
- [5] Ardent D. (2006). Ink Mileage: Measure & Manage [online]. Available from: <http://www.pffc-online.com/process-management/5017-paper-ink-mileage-measure>. [Accessed 20 May 2021].
- [6] Rastetter J., & Bingham J. (2016). Lower Your Anilox Line Screen and Cell Volume for Better Performance FlexoGlobal [online]. Available from: <http://www.flexoglobal.com/blog/2016/08/01/pamarco-lower-anilox-line-screen-cell-volume/>. [Accessed 20 May 2021].
- [7] Teufler S. (2010). Weighing Your Coating Options [online]. Available from: <http://www.harperimage.com/media/downloads/Weighing%20Your%20Coating%20Options%20FLEXO%20Feb%202010.pdf>. [Accessed 22 May 2021].
- [8] Teufler S. (2015). Anilox Rollers - Choosing the Right Lineature [online]. Available from: http://www.harperimage.com/media/downloads/Anilox%20Rollers_Choosing%20The%20Right%20Lineature_Flexible%20Packaging%20Issue%201.pdf. [Accessed 22 May 2021].
- [9] Hogan P. (2018). Aniloxes - Yesterday, Today and Tomorrow [online]. Available from: http://www.harperimage.com/media/downloads/Aniloxes_Yesterday%20Today%20and%20Tomorrow_%20L&NW%20NovDec%202018.pdf. [Accessed 22 May 2021].
- [10] Harper C. (2005). Do you know what ink film thickness is transferred [online]. Available from: http://www.harperimage.com/media/downloads/Harper_FGA_1_2005.pdf. [Accessed 22 May 2021].
- [11] Green C. (2013). Understanding Common Flexo Print Defects - Part 2 FlexoGlobal [online]. Available from: <http://www.flexoglobal.com/blog/tag/anilox/page/4/>. [Accessed 22 May 2021].
- [12] Poulson B. & Hudson K. (2010). Correlating Ink Labs Drawdown to Press [online]. Available from: <http://www.harperimage.com/media/downloads/Radtech%20Report%20Sep-Oct%202010.pdf>. [Accessed 24 May 2021].
- [13] Harnandez R. (2019). Releasing the Anilox's Power [online]. Available from: http://www.harperimage.com/media/downloads/Releasing%20Anilox%20Power_FLEXO%20Jan%202019.pdf. [Accessed 24 May 2021].
- [14] Olson, R., Yang, L. Stam J. V., & Lesrelius, M. (2006). Effects of ink setting flexographic printing: Coating polarity and dot gain. *Nordic Pulp and Paper Research Journal*, 21(5), 569–574.
- [15] Gencoglu, E. N. (2012). Influence of Ink Viscosity on Dot Gain and Print Density in Flexography. *Asian Journal of Chemistry*, 24(5), 1999–2002.
- [16] Theopold, A., Neumann, J., Massfelder, D., & Dörsam, E. (2012). Effects of Solvents on Flexographic Plates. *Advances in Printing and Media Technology*, 39, 159–168.
- [17] Simseker, O. (2011). Investigation of Different Solvents in Flexographic Printing Ink's Effects to Print Quality on Coated and Uncoated Paper. *Asian Journal of Chemistry*, 23(7), 2903–2906.
- [18] Hizir, F.E., & Hardt, D.E. (2014). Effect of Substrate Contact Angle on Ink Transfer in Flexographic Printing [online]. Available from: http://www.comsol.co.in/paper/download/194575/hizir_paper.pdf. [Accessed 26 May 2021].
- [19] Izdebska, J., Podsiadlo, H., & Hari, L. (2012). Influence of Surface Free Energy of Biodegradable Films on Optical Density of Ink Coated Fields of Prints. *Advances in Printing and Media Technology*, 39, 245–252.
- [20] Rong, X., & Keif, M. (2007). A Study of PLA Printability with Flexography. *The Technical Association of the Graphic Arts*, 3, 605–613.
- [21] Mesic, B., Lestelius, M., & Engstrom, G. (2006). Influence of Corona Treatment Decay on Print Quality in Water-borne Flexographic Printing of Low-density Polyethylene-coated Paperboard. *Packaging Technology and Science*, 19(2), 61–70.
- [22] Valdec, D., Zjakić, I., & Milković, M. (2013). The Influence of Variable Parameters of Flexographic Printing on Dot Geometry of Pre-printed Printing Substrate. *Tehnički vjesnik*, 20(4), 659–667.
- [23] Claypole, T.C., Jewell, E.H., & Bould, D.C. (2012). Effects of Flexographic Press Parameters on the Reproduction of Colour Images. *Advances in Printing and Media Technology*, 39, 187–194.
- [24] Gilbert, D.E., & Lee, F. (2008). Flexographic Plate Technology: Conventional Solvent Plates Versus Digital Solvent Plates. *Journal of Industrial Technology*, 24(3), 1–7.
- [25] Bould, D.C., Claypole, T.C., & Bohan, M.F.J. (2004). An Investigation into Plate Deformation in Flexographic Printing. *Journal of Engineering Manufacture*, 218(11), 1499–1511.
- [26] Ebnesajjad, S., & Landrock, A. (2015). Surface Tension and Its Measurement. In: S. Ebnesajjad, 3rd ed. *Adhesives Technology Handbook*. William Andrew, Elsevier Inc, 19–29.

Akshay V. Joshi received Bachelor's and Masters Degree in Printing Engineering from University of Pune, India. He was awarded Ph.D. (Engineering) from Jadavpur University, Kolkata in 2015. Dr. Akshay Joshi is working as Assistant Professor, Printing Engineering Department at P. V. G's College of Engineering & Technology and G. K. Pate (Wani) Institute of Management, Pune, India since

1996. He is Coordinator, Board of Studies and Member, Research and Recognition Committee for Printing Technology at Savitribai Phule Pune University. His area of research is Gravure, Flexo and Flexible Packaging. Dr. Akshay Joshi has published several papers in Journals and guided candidates for Master Program in Printing Engineering and evaluated Ph.D. candidates. He is been

internationally qualified as G7 Expert by Idealliance USA and implemented first G7 calibration for Gravure and Flexography printing processes in India. He is a Life Member of Indian Society for Technical Education.

 <http://orcid.org/0000-0002-8733-1747>

An International Journal of Optimization and Control: Theories & Applications (<http://ijocta.balikesir.edu.tr>)



This work is licensed under a Creative Commons Attribution 4.0 International License. The authors retain ownership of the copyright for their article, but they allow anyone to download, reuse, reprint, modify, distribute, and/or copy articles in IJOCTA, so long as the original authors and source are credited. To see the complete license contents, please visit <http://creativecommons.org/licenses/by/4.0/>.